Demodulation of the simulated periodically non-stationary random signal with Hilbert transform

Ihor Javorskyj[1,2,†], Roman Yuzefovych[1,3,*,†], Oleh Lychak[1,†], Pavlo Semenov[4,†] and Roman Sliepko[1,†]

[1] *Karpenko Physico-mechanical Institute of NAS of Ukraine, 79060, 5 Naukova Str., Lviv, Ukraine*

[2] *Bydgoszcz University of Science and Technology, 85796, 7 Al. Prof. S. Kaliskiego, Bydgoszcz, Poland*

[3] *Lviv Polytechnic National University, 79013, 12 Bandera Str., Lviv, Ukraine*

[4] *Odessa National Maritime University, 65029, 34 Mechnikova Str., Odessa, Ukraine*

Abstract

Demodulation procedure of the periodically non-stationary random signals (PNRSs), with carrier harmonics, modulated by stationary, high-frequency random processes was explained. Band-pass filtration and Hilbert transform were used for separation of spectral components of PNRS and quadratures extraction from amplitude-phase modulated signal. Possibility to extract and right estimate the quadratures of narrow-band high frequency modulation stochastic processes was demonstrated. Presented technology will be useful for vibration-based diagnostics of mechanisms.

Keywords

periodically non-stationary random process, amplitude-phase high-frequency modulations, Hilbert transform, quadratures, stochastic simulation, vibrations

1. Introduction

The effectiveness of investigation of the properties of physical systems and processes based on experimental data on their behavior over time is largely determined by the ability to identify and evaluate their main characteristic features [1–3]. These features are obviously the repeatability and stochasticity of their behavior, and these features appear in the properties of the processes not independently but in interaction. Many processes in geophysics, meteorology, radiophysic signals and technical mechanics are characterized by this behavior [4–6]. Periodically non-stationary random processes (PNRP) are mathematical models describing the complex interaction of repeatability and stochasticity

[7–9]. The methods of analysis of such signals (processes) should obviously include in their structure both periodic functions and purely stationary random processes [10–12], both extreme cases and various models of the interaction of periodicity and stochasticity [13–15]. Vibration signals acquired in machines and mechanisms during diagnostics are one example of such processes [16–18].

Vibration signal can be modeled as the superposition of harmonics with multiple frequencies which are stochastically amplitude- and phase-modulated [19–21]. Simulation of PNRP signal as well as its demodulation procedure involving a Hilbert transform are presented in this article.

2. Simulation model of PNRP signal

For simulation we select the following model [22, 23]:

$$\xi(nh) = \xi_c(nh)\cos\omega_0 nh + \xi_s(nh)\sin\omega_0 nh \,, \tag{1}$$

where ω_0 is base cyclic frequency, λ_0 is a central frequency of high-frequency modulation stochastic process.

The quadratures of modulating process have a following form:

$$\xi_c(nh) = p_c(nh)\cos\lambda_0 nh + p_s(nh)\sin\lambda_0 nh \,, \tag{2}$$

$$\xi_s(nh) = q_c(nh)\cos\lambda_0 nh + q_s(nh)\sin\lambda_0 nh \,, \tag{3}$$

and $\quad Ep_{c,s}(nh) = Eq_{c,s}(nh) = 0, \quad R_p^{c,s}(jh) = Ep_{c,s}(nh)\,p_{c,s}((n+j)h), \quad R_p^c(jh) = R_p^s(jh),$
$R_q^{c,s}(jh) = Eq_{c,s}(nh)\,q_{c,s}((n+j)h), \quad R_q^c(jh) = R_q^s(jh), \quad R_p^c(jh) \neq R_q^c(jh), \quad R_{pq}^{c,s}(jh) = 0,$
$R_{pq}^{cs}(jh) = 0, \; R_p^{cs}(jh) = R_q^{cs}(jh) = 0.$ Assume that quadratures in (2) and (3) have different autocovariance functions, and are non-correlated. The covariance function of (1) is equal to:

$$b_\xi(nh, jh) = B_0^{(\xi)}(jh) + C_2^{(\xi)}(jh)\cos 2\omega_0 nh + S_2^{(\xi)}(jh)\sin 2\omega_0 nh \,,$$

where

$$B_0^{(\xi)}(jh) = \frac{1}{2}\left[R_p^c(jh) + R_q^c(jh)\right]\cos\lambda_0 jh\cos\omega_0 jh \,, \tag{4}$$

$$C_2^{(\xi)}(jh) = \frac{1}{2}\left[R_p^c(jh) - R_q^c(jh)\right]\cos\lambda_0 jh\cos\omega_0 jh \,, \tag{5}$$

$$S_2^{(\xi)}(jh) = \frac{1}{2}\left[R_q^c(jh) - R_p^c(jh)\right]\cos\lambda_0 jh\sin\omega_0 jh \,. \tag{6}$$

Now, let's assume that

$$R_p^c(jh) = A_p e^{-\alpha_p|j|h} \,, \; R_q^c(jh) = A_q e^{-\alpha_p|j|h} \,,$$

For the simulation of PNRP series the following parameter values were used $A_p = 10$, $A_q = 4$, $\alpha_p = \alpha_q = 0.01$, $\omega_0 = 10^2 \pi$, $\lambda_0 = 2 \cdot 10^3 \pi$, series length $K = 5 \cdot 10^4$. A fragment of the simulated series is shown in Fig. 1. The estimators of the covariance components were calculated using the following equations:

$$\hat{B}_0^{(\xi)}(jh) = \frac{1}{K} \sum_{n=0}^{K-1} \xi(nh) \xi((n+j)h),$$

$$\left\{ \begin{matrix} \hat{C}_2^{(\xi)}(jh) \\ \hat{S}_2^{(\xi)}(jh) \end{matrix} \right\} = \frac{2}{K} \sum_{n=0}^{K-1} \xi(nh) \xi((n+j)h) \left\{ \begin{matrix} \cos 2\omega_0 nh \\ \sin 2\omega_0 nh \end{matrix} \right\},$$

are presented in Fig. 2. As we can see, the forms of the estimators behavior and their values have insignificant difference from their theoretical values substituted in (4)–(6).
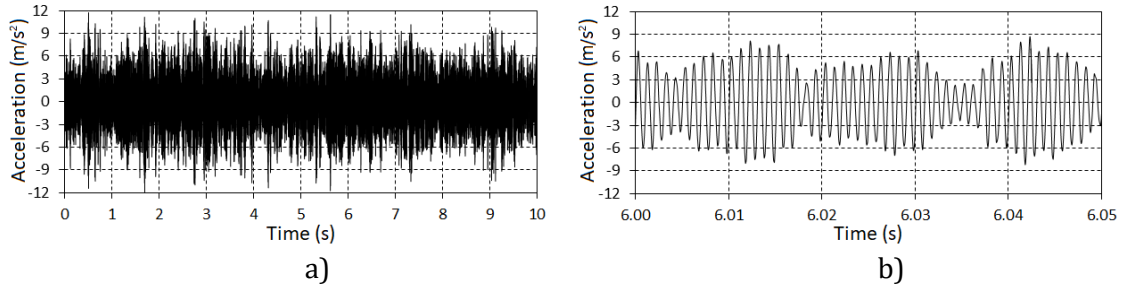
Figure 1: Simulated PNRP series (a) and its local segment (b)
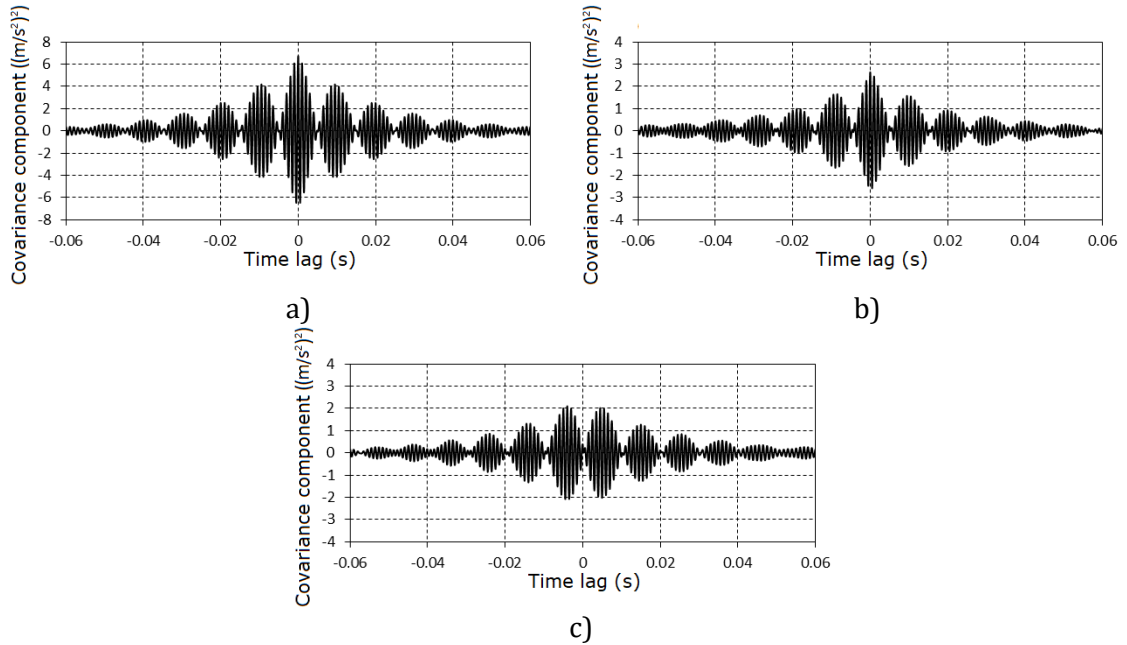
Figure 2: Estimators of the covariance components: (a) $\hat{B}_0^{(\xi)}(u)$; (b) $\hat{C}_2^{(\xi)}(u)$; (c) $\hat{S}_2^{(\xi)}(u)$.

Now let us obtain of the Hilbert transform $H[\bullet]$ for simulated PNRP series [24, 25] $\eta(nh) = H[\xi(nh)]$. Calculations of the estimators of the covariance components based on the Hilbert transform for series

$$\eta(nh) = \eta_c(nh)\cos\omega_0 nh + \eta_s(nh)\sin\omega_0 nh,$$

confirm that the differences between the values of the covariance components for the signal and its Hilbert transform are negligible (Fig. 3).
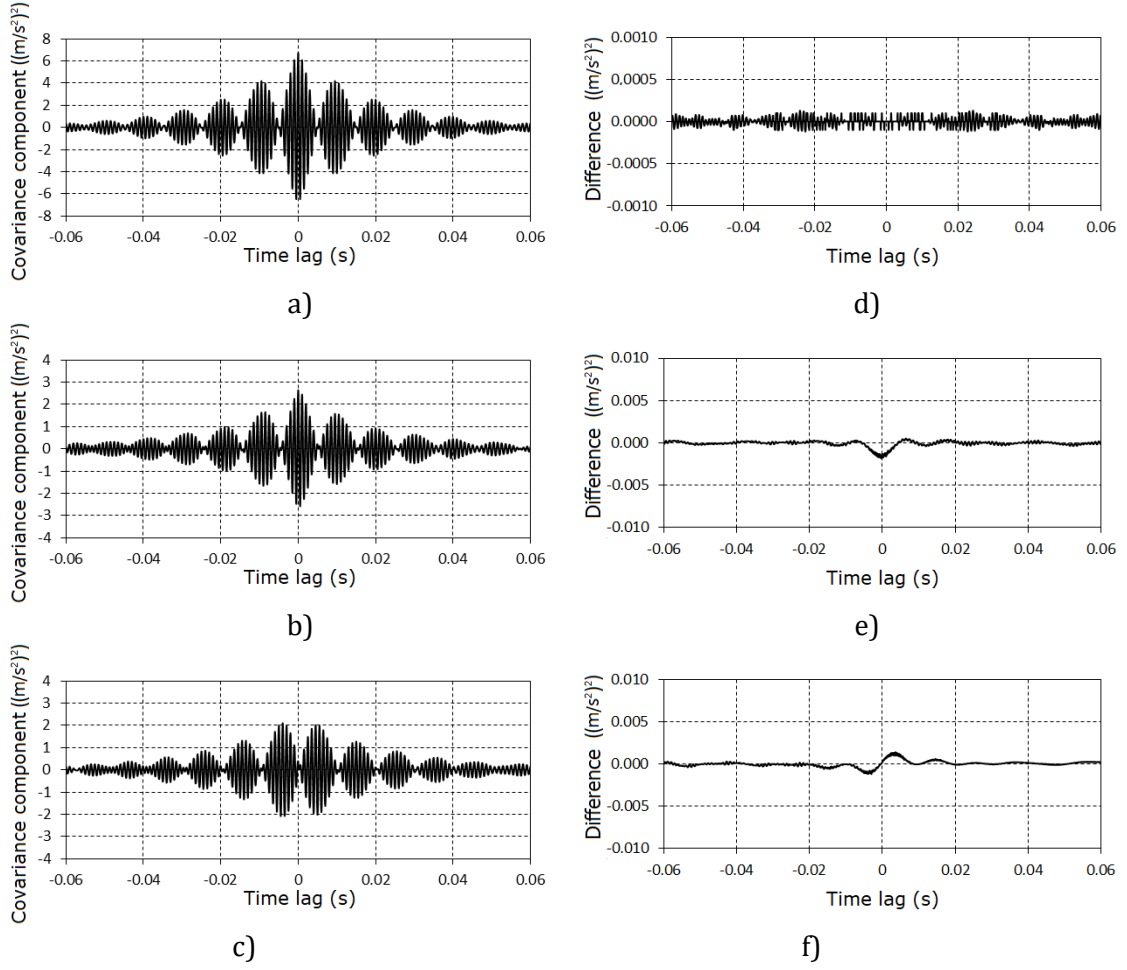
Figure 3: Estimators of the covariance components for the Hilbert transform of simulated series (signal) (a) $\hat{B}_0^{(\eta)}(u)$; (b) $\hat{C}_2^{(\eta)}(u)$; (c) $\hat{S}_2^{(\eta)}(u)$ and differences $\hat{B}_0^{(\xi)}(u) - \hat{B}_0^{(\eta)}(u)$ (d), $\hat{C}_2^{(\xi)}(u) - \hat{C}_2^{(\eta)}(u)$ (e), $\hat{S}_2^{(\xi)}(u) - \hat{S}_2^{(\eta)}(u)$ (f)

The zeroth spectral component for series was estimated using the equation

$$\hat{f}_0(\omega) = \frac{h}{2\pi} \sum_{\eta=-L}^{L} \hat{B}_0^{(\xi)}(nh) k(nh)\cos\omega nh,$$

where $k(nh)$ is the Hamming window, $L=\dfrac{u_m}{h}$, and u_m is the cut-off point of the correlogram.. The graph of $\hat{f}_0(\omega)$ shown in Fig. 4 explains two clear peaks.
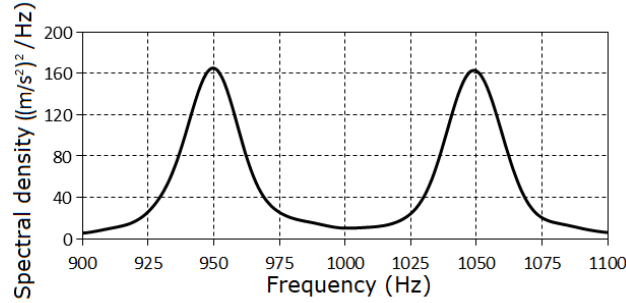
Figure 4: Estimator of the power spectral density zero[th] spectral component for signal

3. Hilbert transform - based demodulation method

To separate two spectral components of PNRP signal [16, 25] we use band-pass filtering with the rectangular transfer functions

$$H_1(\omega)=\begin{cases}1, for\ \dfrac{\omega}{2\pi}\in\left[9\cdot10^2\,Hz,10^3\,Hz\right],\\ 0, for\ other\ frequencies,\end{cases}$$

and

$$H_2(\omega)=\begin{cases}1, for\ \dfrac{\omega}{2\pi}\in\left[10^3\,Hz,11\cdot10^3\,Hz\right].\\ 0, for\ other\ frequencies,\end{cases}$$

Two obtained filtered signals can be represented in the form

$$\xi^+(nh)=\mu_c(nh)\cos(\lambda_0+\omega_0)nh+\mu_s(nh)\sin(\lambda_0+\omega_0)nh, \tag{7}$$

$$\xi^-(nh)=v_c(nh)\cos(\lambda_0-\omega_0)nh+v_s(nh)\sin(\lambda_0-\omega_0)nh, \tag{8}$$

where $\xi^+(nh)$, $\xi^-(nh)$ are upper and lower frequency bands respectively, and

$$\mu_c(t)=\frac{1}{2}\left[p_c(t)-q_s(t)\right],\ \mu_s(t)=\frac{1}{2}\left[q_c(t)+p_s(t)\right],$$

$$v_c(t)=\frac{1}{2}\left[p_c(t)+q_s(t)\right],\ v_s(t)=\frac{1}{2}\left[p_s(t)-q_c(t)\right].$$

The estimators of the autocovariance functions for the series in (7) and (8) are slowly decaying harmonic oscillations (Fig. 5), with frequencies of 950 Hz and 1050 Hz. Obtained estimator values well coincide with the theoretical ones, calculated by the equations:

$$R_{\xi^+}(u) = \frac{1}{4}\left[R_p^c(u) + R_q^c(u)\right]\cos\left(\lambda_0 + \omega_0\right)u,$$

$$R_{\xi^-}(u) = \frac{1}{4}\left[R_p^c(u) + R_q^c(u)\right]\cos\left(\lambda_0 - \omega_0\right)u.$$

The values of the second component estimators for the time series in (7) and (8) for the arbitrary lag are smaller than $1 \cdot 10^{-2}$. Thus, the separated spectral components of (7) and (8) can be considered as realizations of stationary random processes. Note that the sum of their autocovariance functions is equal to the zero covariance components in (4).

a)   b)
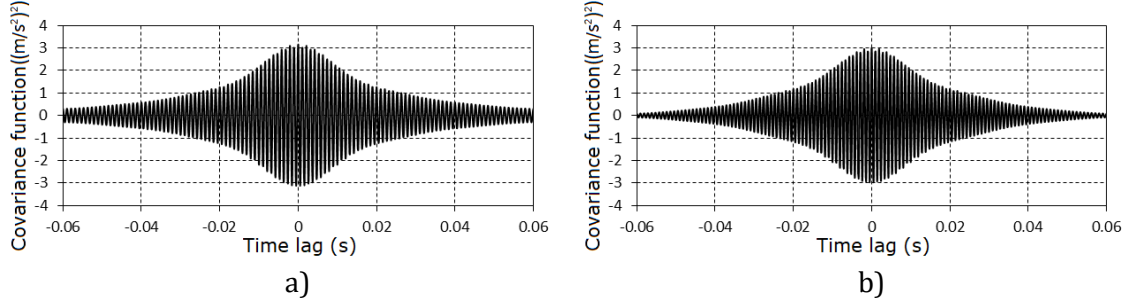
Figure 5: Estimators of the covariance functions of the separated components
(a) $\hat{R}_{\xi^-}(u)$; (b) $\hat{R}_{\xi^+}(u)$

The cross-covariance functions of (7) and (8), are calculated as following:

$$R_{\xi^+\xi^-}(t,u) = \frac{1}{4}\left[R_p^c(u) - R_q^c(u)\right]\cos\left[2\omega_0 t - (\lambda_0 - \omega_0)u\right],$$

$$R_{\xi^-\xi^+}(t,u) = \frac{1}{4}\left[R_p^c(u) - R_q^c(u)\right]\cos\left[2\omega_0 t + (\lambda_0 + \omega_0)u\right],$$

It is clear that $R_{\xi^-\xi^+}(t,u) = R_{\xi^+\xi^-}(t+u,-u)$. Using following statistics:

$$\left\{ \begin{matrix} \hat{C}_2^{\xi^+\xi^-}(jh) \\ \hat{S}_2^{\xi^+\xi^-}(jh) \end{matrix} \right\} = \frac{2}{K}\sum_{n=0}^{K-1}\xi^+(nh)\xi^-\left((n+j)h\right)\left\{ \begin{matrix} \cos 2\omega_0 nh \\ \sin 2\omega_0 nh \end{matrix} \right\},$$

$$\left\{ \begin{matrix} \hat{C}_2^{\xi^-\xi^+}(jh) \\ \hat{S}_2^{\xi^-\xi^+}(jh) \end{matrix} \right\} = \frac{2}{K}\sum_{n=0}^{K-1}\xi^-(nh)\xi^-\left((n+j)h\right)\left\{ \begin{matrix} \cos 2\omega_0 nh \\ \sin 2\omega_0 nh \end{matrix} \right\},$$

we can estimate of the second cosine and sine harmonics [22] for the cross-covariance functions of (7) and (8). Summing these quantities, we obtain the estimators of the covariance components in (5) and (6), respectively, as shown in Fig. 2:

$$\hat{C}_2^{\xi^+\xi^-}(jh) + \hat{C}_2^{\xi^-\xi^+}(jh) = \hat{C}_2^{\xi}(jh),$$

$$\hat{S}_2^{\xi^+\xi^-}(jh) + \hat{S}_2^{\xi^-\xi^+}(jh) = \hat{S}_2^{(\xi)}(jh).$$

A Hilbert transform of the processes in (7) and (8) gives:

$$\eta^+(nh) = \mu_c(nh)\sin(\lambda_0 + \omega_0)nh - \mu_s(nh)\cos(\lambda_0 + \omega_0)nh,$$

$$\eta^-(nh) = v_c(nh)\sin(\lambda_0 - \omega_0)nh - v_s(nh)\cos(\lambda_0 - \omega_0)nh,$$

and then we can extract of their quadratures as following:

$$\mu_c(nh) = \xi^+(nh)\cos(\lambda_0 + \omega_0)nh + \eta^+(nh)\sin(\lambda_0 + \omega_0)nh,$$

$$\mu_s(nh) = \xi^+(nh)\sin(\lambda_0 + \omega_0)nh - \eta^+(nh)\cos(\lambda_0 + \omega_0)nh,$$

$$v_c(nh) = \xi^-(nh)\cos(\lambda_0 - \omega_0)nh + \eta^-(nh)\sin(\lambda_0 - \omega_0)nh,$$

$$v_s(nh) = \xi^-(nh)\sin(\lambda_0 - \omega_0)nh - \eta^-(nh)\cos(\lambda_0 - \omega_0)nh.$$

The segments of the quadrature time series are shown in Fig. 6. The estimators of the covariance functions of the quadratures for $\xi^-(t)$ are presented in Fig. 7. These are slowly decaying functions. Small differences between their values and the theoretical ones, which were determined by the relations:

$$R_\mu^c(u) = \frac{1}{4}\left[R_p^c(u) + R_q^s(u)\right], \ R_\mu^s(u) = \frac{1}{4}\left[R_p^s(u) + R_q^c(u)\right],$$

$$R_v^c(u) = \frac{1}{4}\left[R_p^c(u) + R_q^s(u)\right], \ R_v^s(u) = \frac{1}{4}\left[R_p^s(u) + R_q^c(u)\right],$$

can be explained by statistical errors of calculations.
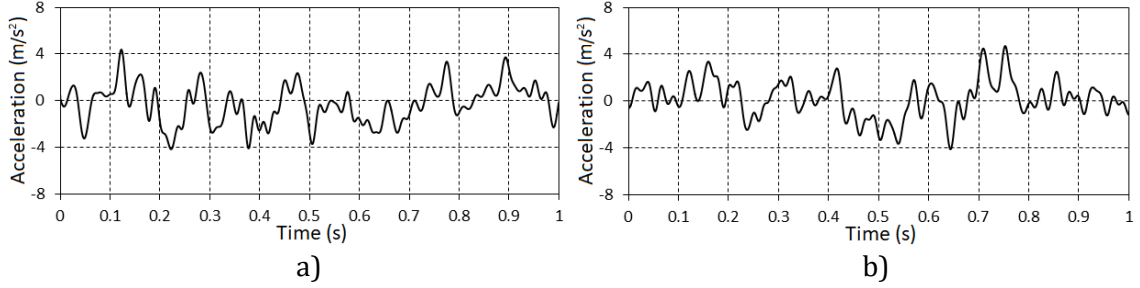
Figure 6: Cosine (a) and sine (b) quadratures for the component $\xi^-(t)$
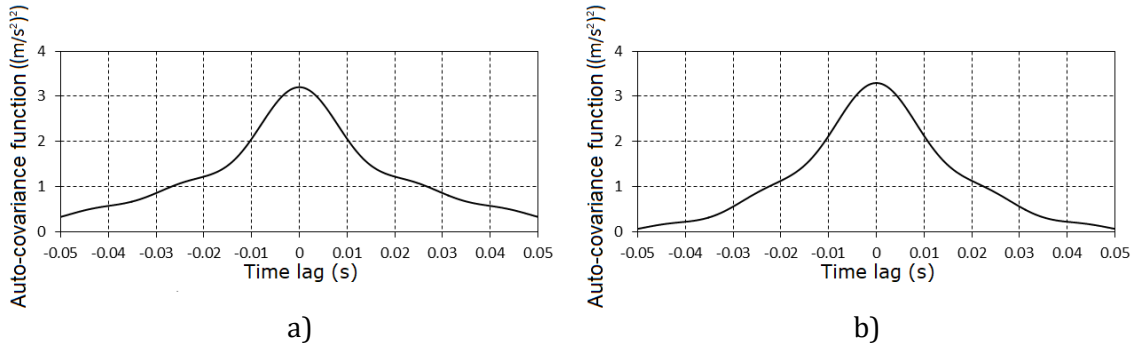
Figure 7: Autocovariance functions of the (a) cosine and (b) sine quadratures for $\xi^-(t)$

The results of calculations of the cross-covariance functions shown on Figs. 8 and 9

$$\hat{R}_{\mu}^{cs}\left(jh\right)= \frac{1}{K}\sum_{n=0}^{K-1}\mu_c\left(nh\right)\mu_s\left(\left(n+j\right)h\right), \ \hat{R}_{v}^{cs}\left(jh\right)= \frac{1}{K}\sum_{n=0}^{K-1}v_c\left(nh\right)v_s\left(\left(n+j\right)h\right),$$

$$\hat{R}_{\mu v}^{cs}\left(jh\right)= \frac{1}{K}\sum_{n=0}^{K-1}\mu_c\left(nh\right)v_s\left(\left(n+j\right)h\right), \ \hat{R}_{v\mu}^{cs}\left(jh\right)= \frac{1}{K}\sum_{n=0}^{K-1}v_c\left(nh\right)\mu_s\left(\left(n+j\right)h\right)$$

confirm that the respective quadratures are non-correlated.

a)

b)
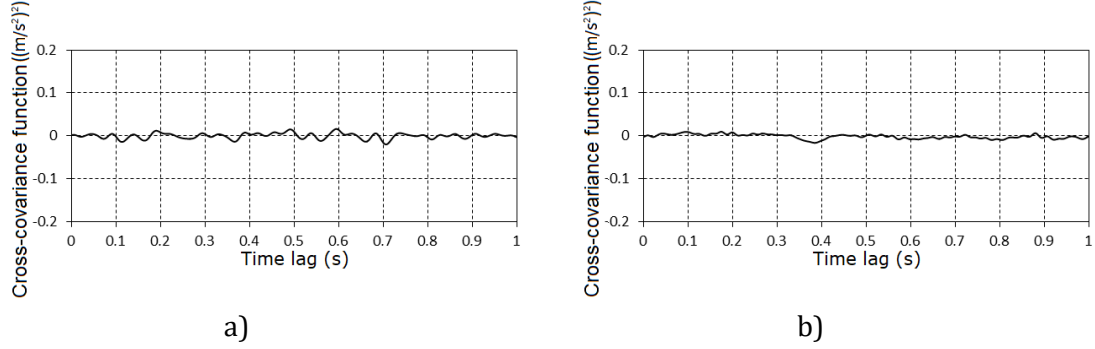
Figure 8: Cross-covariance functions of the quadratures for each component: (a) $\hat{R}_{v}^{cs}\left(u\right)$; (b) $\hat{R}_{\mu}^{cs}\left(u\right)$

a)

b)
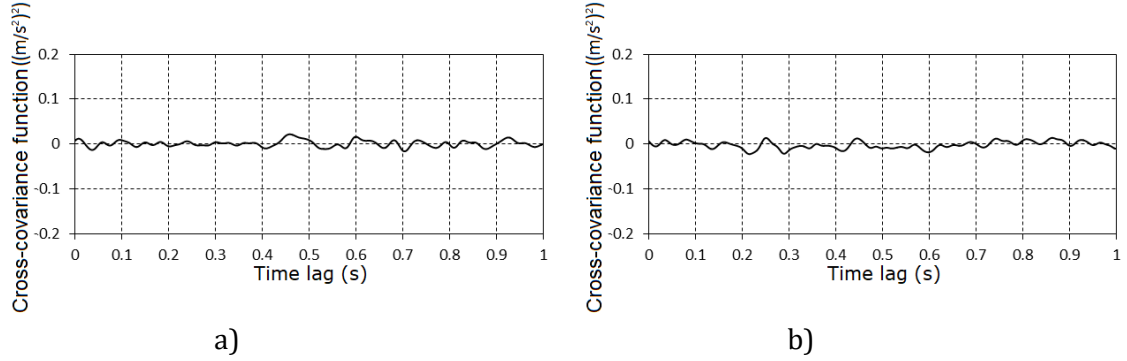
Figure 9: Cross-covariance functions of the quadratures for different components: (a) $\hat{R}_{\mu v}^{cs}(u)$; (b) $\hat{R}_{\mu v}^{sc}(u)$

4. Conclusion

Demodulation of the simulated PNRP with Hilbert transform-based procedures approved that it is possible to extract quadratures of the modulating processes and right estimate their covariance properties with statistically satisfied accuracy. Such processing technology can be useful for demodulation of the complex vibration signals for diagnostics of mechanisms.

References

[1] V. Kyryliv, Ya. Kyryliv, N. Sas, Formation of surface ultrafine grain structure and their physical and mechanical characteristics using vibration-centrifugal hardening, Advances in Materials Science and Engineering, 2018, Article number 3152170. doi: 10.1155/2018/3152170.

[2] I. Dolinska, Evaluation of the residual service life of a disk of the rotor of steam turbine with regard for the number of shutdowns of the equipment, Mater. Sci. 53(5) (2018) 637–644. doi: 10.1007/s11003-018-0118-y.

[3] A. M. Syrotyuk, A. V. Babii, R. A. Barna, R. L. Leshchak, P. O. Marushchak, Corrosion-Fatigue crack-growth resistance of steel of the frame of a sprayer boom, Mater. Sci. 56(4) (2021) 466–471. doi: 10.1007/s11003-021-00452-2.

[4] J. S. Bendat, A. G. Piersol, Random data: Analysis and measurement procedures, John Wiley & Sons, Ltd., 2010.

[5] W. A. Gardner, Cyclostationarity in Communications and Signal Processing, IEEE Press, New York, 1994.

[6] J. Antoni, Cyclostationarity by examples, Mech. Syst. Signal Process. 23 (2009) 987–1036. doi: 10.1016/j.ymssp.2008.10.010.

[7] A. Napolitano, Cyclostationary processes and time series: Theory, applications, and generalizations, Elsevier, Academic Press, 2020.

[8] R. B. Randall, N. Sawalhi, M. Coats, A comparison of methods for separation of deterministic and random signals, Int. J. Cond. Monitoring 1 (2011) 11–19. doi: 10.1784/204764211798089048

[9] R. B. Randall, J. Antoni, S. Chobsaard, The relation between spectral correlation and envelope analysis, Mech. Syst. Signal Process., 15 (5) (2001) 945–962, 2001. doi: org/10.1006/mssp.2001.1415

[10] I. Javorskyj, I. Matsko, R. Yuzefovych, O. Lychak, R. Lys, Methods of hidden periodicity discovering for gearbox fault detection, Sensors 21 (2021) 6138. doi: 10.3390/s21186138.

[11] H. L. Hurd, A. Miamee, Periodically Correlated Random Sequences: Spectral Theory and Practice. Wiley, New York, 2007. doi: 10.1002/9780470182833.

[12] R. Yuzefovych, I. Javorskyj, O. Lychak, P. Semenov, Method of periodically non-stationary random signals demodulation with Hilbert transform, CEUR Workshop Proceedings, 3rd International Workshop on Information Technologies: Theoretical and Applied Problems, ITTAP 2023, 3628 (2023) pp. 548–553.

[13] R. B. Randall, J. Antoni. Rolling element bearing diagnostics—A tutorial. Mech Syst Signal Process. 25(2) (2011) 485–520. doi: 10.1016/j.ymssp.2010.07.017.

[14] L. H. Koopmans, The spectral analysis of time series, New York: Academic Press; 1974.

[15] R. B. Randall, N. Sawalhi, M. Coats, A comparison of methods for separation of deterministic and random signals, Int. J. Cond. Monitoring 1(1) (2011) 11–19. doi: 10.1784/204764211798089048

[16] I. Javorskyj, R. Yuzefovych, I. Matsko, P. Kurapov, Hilbert transform of a periodically non-stationary random signal: Low-frequency modulation, Digit. Signal Process. 116 (2021) 103113. doi: 10.1016/j.dsp.2021.103113

[17] P. Borghesani, P. Pennacchi, R.B. Randall, N. Sawalhi, R. Ricci, Application of cepstrum pre-whitening for the diagnosis of bearing faults under variable speed conditions, Mech. Syst. Signal Process. 36 (2) (2013) 370–384. doi: 10.1016/j.ymssp.2012.11.001

[18] Z. K. Zhu, Z. H. Feng, F. R. Kong, Cyclostationarity analysis for gearbox condition monitoring: Approaches and effectiveness, Mech. Syst. Signal Process., 19(3) (2005) 467–482. doi: 10.1016/j.ymssp.2004.02.007.

[19] D. Ho, R. B. Randall, Optimization of bearing diagnostic techniques using simulated and actual bearing fault signals, Mech. Syst. Signal Process. 14(5) (2000) 763–788. doi: 10.1006/mssp.2000.1304.

[20] S. Tyagi, S. K. Panigrahi, An improved envelope detection method using particle swarm optimisation for rolling element bearing fault diagnosis, J. Comput. Des. Eng. 4 (2017) 305–317. doi: 10.1016/j.jcde.2017.05.002.

[21] H. Konstantin-Hansen, Envelope analysis for diagnostics of local faults in rolling element bearings, Denmark: Bruel & Kjaer Application Note, BD0501; 2003.

[22] I. Javorskyj , R. Yuzefovych, O. Lychak, I. Matsko, Hilbert transform for covariance analysis of periodically nonstationary random signals with high-frequency modulation, ISA Transactions 144 (2024) 452–481. doi: 10.1016/j.isatra.2023.10.025

[23] I. Javorskyj , R. Yuzefovych, O. Lychak, R. Sliepko, P. Semenov, Hilbert transform for analysis of amplitude modulated wide-band random signals. Proceedings of XII International Conference on Advanced Computer Information Technologies, ACIT-2022, pp. 68–71. doi: 10.1109/ACIT54803.2022.9913131

[24] S. M. Kay, Modern spectral estimation: Theory and application, New Jersey: Prentice Hall, Englewood Cliffs; 1988.

[25] E. Bedrosian, A product theorem for Hilbert transforms. In: Proceedings of the 51th IEEE. 1963; pp. 868–869. doi: 10.1109/PROC.1963.2308.